

Quantum gates using electronic and nuclear spins of Yb^+ in a magnetic field gradient

K.L. Wang^{1,2,a}, M. Johanning³, M. Feng¹, F. Mintert⁴, and C. Wunderlich³

¹ State Key Laboratory of Magnetic Resonance and Atomic and Molecular Physics, Wuhan Institute of Physics and Mathematics, Chinese Academy of Sciences, and Wuhan National Laboratory for Optoelectronics, Wuhan 430071, P.R. China

² Graduate School of the Chinese Academy of Sciences, Beijing 100049, P.R. China

³ Fachbereich Physik, Universität Siegen, 57068 Siegen, Germany

⁴ Freiburg Institute for Advanced Studies, Albert-Ludwigs-Universität Freiburg, Albertstraße 19, 79104 Freiburg, Germany

Received 17 February 2011 / Received in final form 25 March 2011

Published online 17 May 2011 – © EDP Sciences, Società Italiana di Fisica, Springer-Verlag 2011

Abstract. An efficient scheme is proposed to carry out gate operations on an array of trapped Yb^+ ions, based on a previous proposal using both electronic and nuclear degrees of freedom in a magnetic field gradient. For this purpose we consider the Paschen-Back regime (strong magnetic field) and employ a high-field approximation in this treatment. We show the possibility to suppress the unwanted coupling between the electron spins by appropriately swapping states between electronic and nuclear spins. The feasibility of generating the required high magnetic field is discussed.

1 Introduction

Quantum computing (QC) based on nuclear spins has attracted considerable interest over the past decades due to the long coherence time of nuclear spins. Since they only weakly interact with their environment, nuclear spins are well suited for storing quantum information, and, for the same reason, difficult to manipulate. As a result, to carry out QC, one may work with ensembles of nuclear spins [1] or employ a hyperfine interaction to manipulate individual nuclear spins by electron spins [2]. The former, using mature techniques of nuclear magnetic resonance, has become a test bed for models and schemes of QC and quantum simulations [3,4], while the exploitation of the latter is still at an early stage.

Furthermore, there have been proposals combining nuclear and electronic spins in solid-state systems, such as doped silicon substrates [5] and doped fullerenes [6,7]. To distinguish nuclear and electronic degrees of freedom, one has to introduce a strong magnetic field and work in the Paschen-Back regime. An experimental demonstration of the manipulation of a nuclear spin ensemble with about 10 000 ions in a Penning trap under magnetic field 0.8 T was reported by Bollinger et al. [8]. The manipulation of individual nuclear spins had only been achieved in diamond nitrogen-vacancy centers, with qubits encoded in the ^{13}C or ^{15}N nuclear spins near the electron spin [9,10].

Here, we propose a scheme, using trapped $^{171}\text{Yb}^+$ ions, to encode qubits in both electronic and nuclear spins of

trapped atomic ions for QC and quantum simulations, following a previous idea [11]. Different from already accomplished experimental work with trapped ions [12,13], we consider quantum logic operations on ions in the Paschen-Back regime with qubits encoded in nuclear spins I and auxiliary qubits in electron spins $S = 1/2$. This combines the long decoherence time of nuclear spins with efficient manipulation and readout using electron spins. Quantum information is stored in nuclear spins and is only swapped into electronic spins for single-qubit gates and conditional quantum dynamics with two and more ions. Thus, quantum information remains well protected from ambient noise fields that otherwise would give rise to decoherence.

Swapping quantum information between nuclear and electron spins is accomplished using microwave radiation. Subsequent conditional quantum dynamics between electron spins and individual addressing of electron spins may be done using laser light [14,15], or, in the presence of a spatially varying magnetic field, using again microwave radiation [16–23]. A magnetic field gradient induces spin-spin coupling [19–21] between electronic spins that can be used for quantum logic gates, and, in addition allows for ions to be addressed in frequency space. The latter approach is useful, since it avoids technical and fundamental difficulties when using laser light for coherent operations [17,18,20,22,24]. In addition, it allows for conditional quantum dynamics without stringent requirements on the cooling of the ions' vibrational motion [25].

The key point of our proposal is the suppression of unwanted coupling between electronic spins in the magnetic

^a e-mail: LynneWang@gmail.com

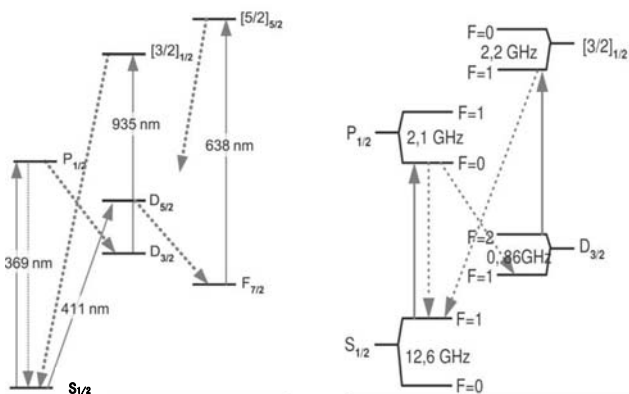


Fig. 1. Energy-level schemes of $^{172}\text{Yb}^+$ (left) and $^{171}\text{Yb}^+$ (right), where the energy gaps are not drawn to scale.

field gradient by swapping quantum information between nuclear and electron spins by microwave radiation. As a result, the overhead operations, such as refocusing pulses, in [11] is no longer necessary. In what follows, we first investigate the use of nuclear and electron spins of atomic ions with and without the high-field approximation, from which we know how well the quantum gate is performed in the real experimental situation. Also, a spatially varying magnetic field is included. Then we show how two-qubit gating is achieved without the need for compensating for unwanted couplings between electron spins. Furthermore, a detailed discussion of how the required magnetic field and the magnetic gradient can be achieved is given.

For concreteness, the present work considers as an example the use of $^{171}\text{Yb}^+$ ions for quantum information science [21,26–31]. $^{171}\text{Yb}^+$ features a nuclear spin of one half and thus provides the simplest hyperfine structure with several potential qubits where the experimenter can choose both magnetically sensitive and insensitive qubit transitions (to first order). The hyperfine qubits can be directly manipulated by a resonant microwave field or by using an optical Raman transitions. Recent interest in trapping Yb^+ is, to some extent, motivated also by the fact that the experimenter benefits from low priced diode lasers for photoionization [32] and for all transitions relevant to Doppler cooling, qubit initialization and state selective detection (see Fig. 1).

The paper is structured in four sections. In Section 2 we present the Hamiltonian describing a linear Coulomb crystal of ions and justify the high-field approximation. In Section 3 we will demonstrate efficient QC operations using both nuclear and electron spins, the experimental feasibility of which is discussed in detail in Section 4. We give a brief summary in the last section.

2 The system and the Hamiltonian

We consider an array of trapped ions in a linear trap in the presence of a magnetic field gradient, whose Hamiltonian

in units of $\hbar = 1$ is written as,

$$H = \sum_i \Omega_S^i S_z^i + \sum_i \Omega_I^i I_z^i + A \sum_i (S_x^i I_x^i + S_y^i I_y^i + S_z^i I_z^i) - \frac{1}{2} \sum_{i < j} J_{ij} \hat{S}_z^i \hat{S}_z^j, \quad (1)$$

where S_k and I_k ($k = x, y, z$) are, respectively, the spin operators of the electron spin ($S = 1/2$) and the nuclear spin I . For $^{171}\text{Yb}^+$ we have $I = 1/2$, the hyperfine coupling constant is $A = 12.645$ GHz and the Larmor frequencies are given by $\Omega_S = g_S \mu_B B = 28B$ GHz and $\Omega_I = g_n \mu_B B = -7.5B$ MHz with B the strength of the magnetic field in tesla experienced by the ion. J_{ij} is the coupling between the electron spins of the trapped ions under the magnetic field gradient [19–21]. We leave out the vibrational modes here, because additional radiation fields applied to swap information between nuclear and electron spins only drives carrier transitions, that is, these fields do not couple vibrational and spin states. The nuclear spin couplings are also neglected as they are very small compared to other terms.

The magnetic field is applied along the trap axis, so the i th ion experiences the magnetic field with

$$\mathbf{B} = [B_0 + bz] \hat{e}_z,$$

with B_0 the strength of the magnetic field at the origin, $b = \partial B / \partial z$ the magnetic field gradient, and \hat{e}_z the unit vector along the trap axis. For the spin-spin coupling we have

$$J_{ij} = \sum_{l=1}^N \frac{2}{m\nu_l^2} D_{il} D_{jl} \frac{\partial \Omega_S^i}{\partial z} \frac{\partial \Omega_S^j}{\partial z}, \quad (2)$$

where m is the mass of trapped ions, $\nu_l^2 = \nu_z^2 \mu_l$ with ν_z the axial frequency of the trap and μ_l the eigenvalue of potential Hessian matrix. D is the unitary transformation matrix that diagonalizes the Hessian matrix and Ω_S^i depends on magnetic gradient b . With respect to the original expression of J_{ij} in [20,21], equation (2) seems formally larger by 4 times, which is because we use angular momentum operators here instead of the Pauli operators.

For our purpose, we first consider the single-ion case to justify the high-field treatment. In the Paschen-Back regime, the Hamiltonian of a single ion is obtained by reducing equation (1),

$$H_0 = \Omega_S S_z + \Omega_I I_z + A(S_x I_x + S_y I_y + S_z I_z). \quad (3)$$

Assuming a magnetic field $B = 1$ T, we plot the energy-level structure determined by equation (3) in Figure 2 for $^{171}\text{Yb}^+$, where the eigenstates include some superpositions due to the x - and y -terms of the hyperfine interaction. In contrast, the conventional treatment, to simplify the problem, is the exclusion of the x - and y -terms of the hyperfine interaction under the high-field approximation, i.e.,

$$H_1 = \Omega_S S_z + \Omega_I I_z + A S_z I_z. \quad (4)$$

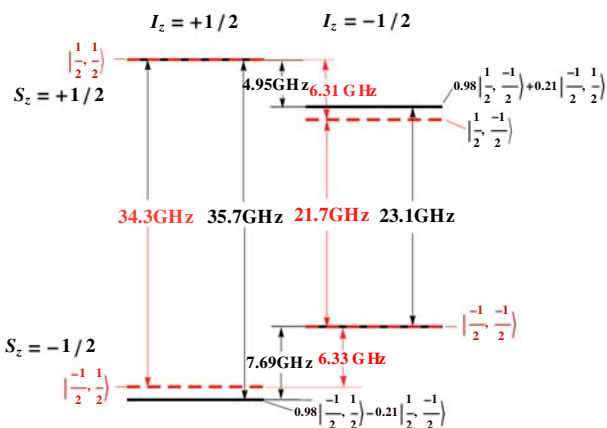


Fig. 2. (Color online) Angular momentum states in the ground state of a $^{171}\text{Yb}^+$ ion in a magnetic field $B = 1$ T (i.e. in the Paschen-Back regime). The levels drawn with the black solid lines and the red dashed lines are, respectively, from the exact Hamiltonian equation (3) and the approximated Hamiltonian equation (4).

Since each term in this Hamiltonian is diagonal, the eigenstates of the Hamiltonian are ones of S_z or I_z .

In order to carry out single-qubit gates and conditional quantum gates with nuclear spins (that are used as a quantum memory), it is necessary to transfer the nuclear spin's state to the electron spin and vice versa. Since the SWAP gate could be performed by appropriate CNOT gate sequences, e.g., $\text{SWAP} = \text{CNOT}_{IS}\text{CNOT}_{SI}\text{CNOT}_{IS} = \text{CNOT}_{SI}\text{CNOT}_{IS}\text{CNOT}_{SI}$ [11] with CNOT_{ab} implying the control a and target b , we consider below the necessary CNOT gates, which could be accomplished by radiating the ion with appropriate π pulses [11]. The key point is the consideration of the level shifts due to hyperfine interaction.

Taking a CNOT_{SI} gate as an example, under the high-field approximation with the magnetic field 1 T, we may radiate the ion by a 6.31 GHz microwave pulse, yielding the flip between $|1/2, 1/2\rangle$ and $|1/2, -1/2\rangle$ (see energy levels in red by dashed lines in Fig. 2). This pulse does not lead to transitions between the levels $|-1/2, 1/2\rangle$ and $|-1/2, -1/2\rangle$ due to detuning. As a result, the flip of the nuclear spin is controlled by the electronic spin. The idea is easily extended to perform a CNOT_{IS} with the nuclear spin as the control qubit. If the exact treatment is used instead of the high-field approximation, however, the involvement of x - and y -terms of hyperfine interaction in equation (3) makes the CNOT gates considered above less perfect.

As shown by the black solid lines in Figure 2, to achieve the transition $|1/2, 1/2\rangle \leftrightarrow |1/2, -1/2\rangle$, we may employ the pulse with frequency 4.95 GHz, which actually leads to

$$|1/2, 1/2\rangle_{ex} \leftrightarrow 0.9776|1/2, -1/2\rangle_{ex} + 0.2103|-1/2, 1/2\rangle_{ex},$$

where $|\dots\rangle_{ex}$ means the state under exact evolution. So the ion would leak to the unwanted state $|-1/2, 1/2\rangle$ state with probability 0.04.

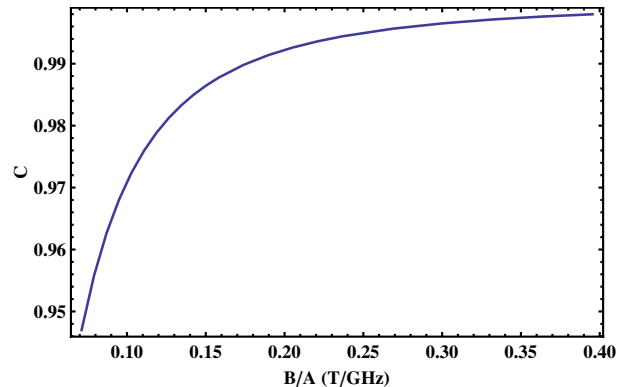


Fig. 3. (Color online) Fidelity C of the CNOT_{SI} gating with respect to the magnetic field strength B divided by hyperfine coupling constant A . Here $C = |\langle \Psi | \Psi_{exact} \rangle|^2$ with $|\Psi\rangle$ and $|\Psi_{exact}\rangle$ the evolved wavefunctions under equation (5) with effective Larmor frequencies and under equation (3). This result with scaled magnetic field can be applied to other ions with $I = 1/2$ and $S = 1/2$ in a good approximation (i.e., neglecting the difference between nuclear Larmor frequencies of different ions). For $^{171}\text{Yb}^+$, the magnetic field changes within the range (0.9 T, 5 T).

To have a preferable quantum gate in a realistic experiment under the high-field approximation, we have to first justify the condition for equation (4). To this end, we require the level splittings under the high-field approximation to be identical to the exact situation, which makes the theoretical treatment closer to the realistic operation. So we introduce effective gyromagnetic ratios to replace the natural gyromagnetic ratios in the treatment of equation (4). By numerics, we have found the effective Larmor frequencies should be,

$$\Omega'_S \approx \gamma'_S B_0 \text{ GHz}$$

and

$$\Omega'_I \approx -\gamma'_I B_0 \text{ GHz}$$

for $1 \text{ T} < B_0 < 5 \text{ T}$. Effective gyromagnetic ratios read $\gamma'_S \approx (28.1 + 5.5e^{-1.5B_0/B_1})$ and $\gamma'_I \approx -(0.085 + 5.5e^{-1.5B_0/B_1})$ (with $B_1 = 1 \text{ T}$). With these effective Larmor frequencies, equation (4) becomes

$$H_1 = \Omega'_S S_z + \Omega'_I I_z + A S_z I_z. \quad (5)$$

Equation (5) is a good approximation to equation (3) which gives nearly the same energy levels. In Figure 3 we show a higher fidelity is achieved for a CNOT gate with increasing magnetic field.

From now on we use the approximate Hamiltonian equation (4) with effective Larmor frequencies to simplify the treatment in multi-ion situation. We have to emphasize that the purpose of the approximation we employ is, on the one hand, to keep consistent with the conventional treatments in previous works [6,7,11], on the other hand, to have a clear physical picture for our gate operations. Since the nuclear and electronic spins are never completely decoupled in real case, we justified the approximation in the above treatment to try to find a trade-off for achieving accurate and coherent gate operations.

3 Quantum gating using S-I swap

Consider a string of trapped ions in the presence of a spatially varying magnetic field along the z -direction, as described by equation (1). In the Paschen-Back regime, we may neglect the x - and y -terms in the hyperfine interaction. So the Hamiltonian is reduced to

$$H_2 = \sum_i \Omega_S^i S_z^i + \sum_i \Omega_I^i I_z^i + A \sum_i S_z^i I_z^i - \frac{1}{2} \sum_{i<j} J_{ij} S_z^i S_z^j. \quad (6)$$

The nuclear spins, due to negligible coupling with each other, remain the same as in the single ion case. But we have to pay more attention to the electron spins, which are coupled due to the magnetic field gradient. Because of these J couplings, the transition frequency of a given ion depends on the electron spin states of others. So with an increasing number of ions the spectrum of the ion chain becomes more complex.

A good candidate system for gate operations should have the coupling between qubits well controlled. In the absence of a magnetic field gradient, trapped ionic qubits interact by coupling to the common vibrational modes mediated by suitably tuned laser light [12–15]. Here, in the presence of a magnetic field gradient, the electron spins' coupling, that reaches well beyond nearest neighbors, is to be used for conditional quantum dynamics. Other QC proposals that make use of nuclear and electron spins usually assume only nearest neighbor coupling [6,7]. For our present trapped ion model, however, the interactions between the ions are significantly beyond the nearest neighbor couplings.

Previously proposed solutions to this problem include: (1) refocusing operations applied simultaneously with the gating pulses on the trapped ions [11] and (2) additional potentials applied on the trapped ion [19,33]. The former solution is based on exact knowledge of the undesired coupling, and overhead in this method increases quickly with the number of qubits. The latter requires micro-structured electrodes traps to shape the effective potential confining the ions. In order to produce sizeable J couplings in the system, the electrodes' axial extension should be of the order of 10 micrometers or smaller and the distance between the electrodes' surface and the ions needs to be of similar magnitude.

In what follows we present an alternative approach to accomplish high-fidelity two-qubit gating making use of the two spins available in each trapped ion. Since both the electron spin and the nuclear spin are initially polarized, the quantum information during the QC implementation is only stored in one of them and the other remains well polarized. When an ion is active, i.e., operated for gating or readout, the quantum information is encoded in the corresponding electron spin and the corresponding nuclear spin remains well polarized. When the ion turns passive, the quantum information is swapped to the nuclear spin for storage, and the electronic spin becomes well polarized.

Consider two active ions in an array of ions. Since the electronic spins of all other ions are well polarized and their nuclear spins, encoding the quantum states, have no

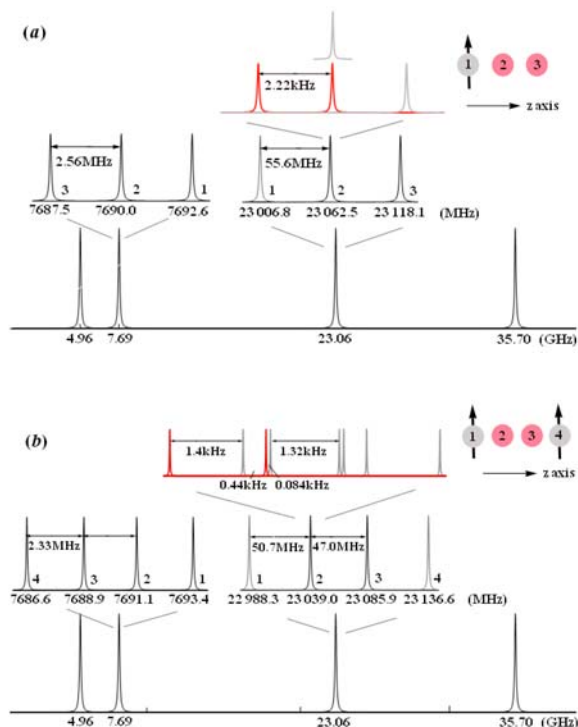


Fig. 4. (Color online) Spectrum of trapped ions with magnetic field $B_0 = 1$ T, field gradient $b = 500$ T/m, and axial trap frequency $\nu_z = 600$ kHz, where (a) is for three ions and (b) for four ions. The lowest trace extends over all resonances; the middle trace shows the splitting due to a magnetic field gradient, and the upper trace depicts the splitting due to J coupling between the ions. Resonant frequencies are marked in lowest and middle traces, and splittings are labeled in the middle and upper traces (some splittings with no labeling due to symmetry). The ions (Nos. 2 and 3) in red stand for active ions and others in gray for passive ions. The frequency lines in red are the ones left after the passive electronic spins are polarized.

interaction with other ions, the two active electronic spins only experience a frequency shift by the polarized electronic spins of the rest passive ions. Compared to the case with the passive electron spins in arbitrary superposition, this scheme makes the spectra much simpler. As a result, quantum gating would be much easier since refocusing unwanted interactions or operations with locally shaped electrostatic potentials in micro-traps are no longer necessary. In addition, quantum states stored in nuclear spin degrees of freedom are more robust to decoherence than in electronic counterpart, which helps to store quantum information in higher fidelity.

Figure 4 demonstrates the cases with three- and four-ions as examples, where two of them are active and the rest are passive. By polarizing the passive electron spins, there are only two frequency lines left for the active spins, which are shifted with respect to the original positions by corresponding J couplings.

We have simulated the two-qubit gating for three and four $^{171}\text{Yb}^+$ trapped in a line under a magnetic field

Table 1. Two-qubit $\text{CNOT}_{S_1S_2}$ gating time T for three and four trapped $^{171}\text{Yb}^+$ in a strong magnetic field $B_0 = 1$ T with axial trap frequencies $\nu_z = 600$ kHz and 200 kHz for different magnetic field gradients b and distances Δz_{\min} . J represents the nearest neighbor coupling for J_{ij} in equation (6). Datas for 4 ions are regarding the middle two ions. N stands for number of ions.

ν_z (kHz)	N	b (T/m)	Δz_{\min} (μm)	J (kHz)	T (ms)
600	3	50	4.15	0.0444	70.8
	3	100	4.15	0.178	17.7
	3	300	4.15	1.60	1.97
	4	50	3.50	0.0368	85.2
	4	100	3.50	0.147	21.3
	4	300	3.50	1.33	2.37
200	3	50	8.63	0.399	7.87
	3	100	8.63	1.60	1.97
	3	300	8.63	14.38	0.218
	4	50	7.28	0.332	9.47
	4	100	7.28	1.33	2.37
	4	300	7.28	11.94	0.263

gradient, as shown in Table 1. The gating time is dependent on the magnetic field gradient, but not on the magnetic field itself. A stronger magnetic field is required just for a better gate manipulation.

4 Experimental feasibility

In order to implement QC and quantum simulations with nuclear spins of trapped ions as described above, a strong and highly stable magnetic field is required. If conditional quantum dynamics is carried out based on magnetic gradient induced coupling [16–18,20–22] using microwave or radio frequency radiation, instead of laser light, then the applied magnetic field in addition needs to vary spatially. In addition, a magnetic field gradient allows for individual ion addressing in frequency space using rf or microwave radiation [16,23]. Below, we will discuss the feasibility of creating the required strong field using Yb^+ ions as a concrete example.

Qubits may be encoded in the simple hyperfine structure of the isotope $^{171}\text{Yb}^+$. Gradients can be achieved by using permanent magnets, for example, in quadrupole configuration or by using a pair of anti-Helmholtz coils or shaped planar current geometries known from magnetic traps for neutral atoms [34,35]. The field noise can be reduced by superconductive materials [23].

In micro-structured traps (two- and three-dimensional), the required magnetic gradient extends only over a limited volume, and thus does not necessarily require strong fields. The optimization of the field geometry using current carrying micro-structures to reach a maximum gradient with a limited current (or dissipated power) appears not too different from the task of optimizing for maximum field. To reach magnetic fields in the Tesla range, however, massive cooling of the current carrying structures would be necessary.

A three-dimensional ion trap has been designed that allows for generating gradients of up to 100 T/m [33]. Details on this trap will be given elsewhere. For neutral atom trapping, two-dimensional current structures were exploited to create flexible magnetic field configurations and magnetic gradients [34–36]. A good thermal contact between current carrying structures and the substrate allows to efficiently remove any thermal intake due to ohmic heating, resulting in enormous possible current densities of $j_{\max} \approx 10^{11}$ A/m² [36] and allows for versatile and fast switchable fields and gradients. With appropriate cooling of the substrate, we expect gradients in the range of 100–300 T/m to be possible for two-dimensional traps that are currently under development in our laboratory at Siegen.

An alternative straightforward solution for producing *both* strong magnetic fields *and* high magnetic gradients would be a pointed yoke which, in its proximity, would create a combination of both. It is desirable, however, to create homogeneous and inhomogeneous parts independently: the gradient is necessary for the addressing of single ions and the coupling between ionic qubits, but it impedes the efficient cooling of the ion chain as a whole, since the microwave transition, which is also required during cooling to avoid optical pumping would be different for each ion. It can thus be advantageous to switch the gradient on during manipulation only, and set it to zero during cooling, and potentially during read-out. The strong offset field, however, that would indiscriminately shift all resonance frequencies over widely spread frequency bands upon switching, remains on at all times. Therefore, in what follows, we will focus on an independent creation of homogeneous and inhomogeneous magnetic fields.

4.1 Possible approaches to creation of high magnetic fields

Methods to generate strong magnetic fields suitable for ion trap QC include:

- Permanent magnets produce stable and low noise fields, which are simple and inexpensive, but cannot be switched on and off nor be tuned directly – the field on a given point however, could be changed by changing the position or orientation of a magnet.
- Current carrying structures on the other hand can produce time dependent fields, but require high power current supplies, and in most cases stabilization and cooling.
- Superconducting current carriers have a better inherent stability but require a high initial experimental effort and costs for setting up a cryostat, and thereby in the long term exhibit high operating costs.

When using type-II super-conductors [37], the persistence of the magnetic field in superconducting coils is usually viewed as an advantage and reduces ac field noise, which, in terms of coherence time is, of course, desirable. On the other hand, permanent magnets offer intrinsic low field noise and the persistence of superconducting magnets can become an obstacle, in case

one intends to modulate the magnetic field periodically using additional current carrying structures. This can be useful, for instance, in order to insert temporal phases with a homogeneous magnetic field and thus homogeneous or global cooling. Slow variations are possible, but not on the time-scale of the typical repetition rate (order of 100 Hz) of data taking.

For a static and homogeneous offset field, we will focus on permanent magnets, where much progress has been made during the last decades [38]: not only did the maximum remanence of commercially available permanent magnets increase substantially (the remanence of $\text{Nd}_2\text{Fe}_{14}\text{B}$ can reach values of up to $B_r = 1.22$ T [39]), but also progress was made in the task of maximizing the field with a given magnet material by choosing a suitable mounting geometry. Our investigations concerned with the creation of strong magnetic fields, therefore, focus on the usage of optimized magnet arrangements to exceed the surface flux of a single magnet. This can be achieved for example by pole and yoke design or in Halbach arrangements [40,41].

4.2 The Halbach structure

Ideally, a Halbach structure consists of an infinitely long magnetized cylinder of continuously varying magnetization direction with inner diameter r_i and outer diameter r_o . The magnetization of a Halbach dipole points along the angle 2ϕ for an infinitesimal cylinder segment at angle ϕ . This results in a cancelation of fields outside of the cylinder and a homogeneous magnetic field inside the cylinder with the magnitude

$$B = B_r \ln \left(\frac{r_o}{r_i} \right), \quad (7)$$

with B_r being the remanence.

A conclusion for the generation of high magnetic fields can be seen from this idealized analytic expression equation (7) for limited outer dimensions, a smaller inner diameter allows for larger field strength. The trap structure and vacuum housing inside the Halbach cylinder cannot be made arbitrarily small, effectively limiting the achievable field strength.

This structure can be replaced, for the ease of fabrication, by a segmented cylinder, made of N homogeneously magnetized segments, as shown in Figure 5, where the field inside becomes

$$B = B_r \left(\frac{\sin(2\pi/N)}{2\pi/N} \right) \ln \left(\frac{r_o}{r_i} \right), \quad (8)$$

and with $N = 16$ segments one can reach already 97% of the field strength of the idealized case.

The finite length of any real Halbach structure, too, contributes to a reduction of the B field according to

$$B = B_r \ln \left(\frac{r_o}{r_i} \right) - B_r f(z_0), \quad (9)$$

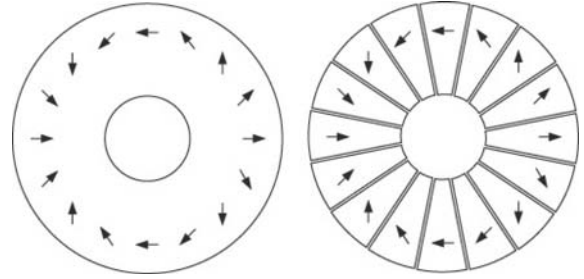


Fig. 5. Schematics for the ideal Halbach configuration (left) and a segmented approximation with $N = 16$ segments (right), which theoretically delivers more than 97% of magnetic field strength in the inner cylinder as compared to the ideal structure. Black arrows indicate the local direction of the magnetic field.

where the reduction factor $f(z_0)$ depends on the length z_0 and the radii r_i and r_o of the cylinder as

$$f(z_0) = \left[\frac{z_0}{2\sqrt{z_0^2 r_o^2}} - \frac{z_0}{2\sqrt{z_0^2 r_i^2}} + \ln \left(\frac{z_0 + \sqrt{z_0^2 r_o^2}}{z_0 + \sqrt{z_0^2 r_i^2}} \right) \right].$$

We carried out numerical simulations for a structure with 16 segments with a cylindrical inner volume of a diameter 5 cm using NdFe35, with a retentivity of $B_r = 1.23$ T. A very homogeneous field of 2.3 T is obtained when the outer diameter is limited to 50 cm (see Fig. 6).

Even stronger fields can be achieved in three-dimensional structures which follow the same concept, namely Halbach spheres, at the expense of constrained optical access to the high-field region [42]. The theoretical field for such an arrangement is given by

$$B = \frac{4}{3} B_r \ln \left(\frac{r_o}{r_i} \right), \quad (10)$$

which is already larger by a factor 1/3 than the field created by a comparable cylinder, but the low optical access makes this choice less attractive, unless the whole detection is placed inside the sphere.

In such structures, the field can exceed the maximum coercivity of the permanent magnet and locally reverse its magnetization (if aligned unfavorably), thus imposing another practical limit on attainable field strengths. This can be avoided, by replacing parts of the magnets with materials with high coercivity (and often lower remanence), and in this way, magnetic fields exceeding 4.5 T have been created [43].

The maximum attainable field strength is limited by material properties as remanence and coercivity, which are usually functions of temperature. For example for NdFeB, the temperature coefficient of the remanence is $-0.1\% \text{ K}^{-1}$, and the temperature coefficient for the coercivity is $-0.6\% \text{ K}^{-1}$, allowing for substantial improvements even if cooling only to liquid nitrogen temperatures [44,45].

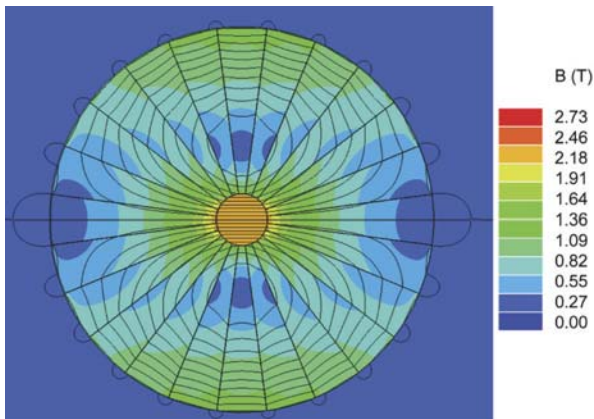


Fig. 6. (Color online) Numerical simulation with a Halbach dipole ring with an inner diameter of 5 cm and an outer diameter of 50 cm, yielding a homogeneous offset field of 2.3 T, in contrast to the analytical model, yielding above 2.8 T. In addition, a set of flux lines is shown.

4.3 Effective potential with magnetic field

Given the substantial strength of magnetic fields considered here, its impact on the ion's motion is a priori not necessarily negligible. To assess the impact of a strong magnetic field, we consider here the dynamics of an ion with mass m and charge e in the presence of both an rf trap potential and a strong magnetic field. An ion's momentum \mathbf{p} is thus replaced by $\mathbf{p} - \frac{e}{m}\mathbf{A}$ with the vector potential \mathbf{A} satisfying $\mathbf{B} = \nabla \times \mathbf{A}$. The exact solution of the equations of motion contains quickly oscillating terms associated with the ion's micro-motion at the frequency Ω_t of the rf trap drive. Averaging over the micro-motion will yield solutions characterized by an effective (pseudo-) potential [46,47].

The Hamiltonian reads $\mathcal{H} = \mathcal{H}_0 + \mathcal{H}_1 \cos \Omega_t t$, with

$$\begin{aligned} \mathcal{H}_0 &= \frac{(\mathbf{p} - e\mathbf{A})^2}{2m} + \frac{1}{8}m\Omega_t^2 a(x^2 + y^2) \\ \text{and} \quad \mathcal{H}_1 &= -\frac{1}{4}m\Omega_t^2 q(x^2 - y^2), \end{aligned} \quad (11)$$

where a and q are the usual stability parameters characterizing the trapping potential [46].

The corresponding Schrödinger equation can be solved with the ansatz

$$\Psi(x, y, t) = \Phi(x, y, t)e^{-i\alpha(t)V_t(x, y)} \quad (12)$$

of a slowly varying wave function $\Phi(x, y, t)$ and the quickly oscillating phase $\alpha = \frac{1}{\hbar\Omega_t} \sin \Omega_t t$. Averaging the time-dependent Schrödinger equation over the interval $\delta t = 2\pi\Omega_t^{-1}$ and taking Φ to be constant over this period yields

$$i\hbar \frac{\partial \Phi}{\partial t} = \mathcal{H}\Phi, \quad (13)$$

with

$$\mathcal{H} = \frac{1}{2m}(p_x^2 + p_y^2) + \frac{1}{2}m\omega_r^2(x^2 + y^2) + \frac{1}{2}\omega_c(p_x y - p_y x) \quad (14)$$

where the following averages have been used: $\frac{\Omega_t}{2\pi} \int_0^{2\pi\Omega_t^{-1}} \alpha dt = 0$, $\frac{\Omega_t}{2\pi} \int_0^{2\pi\Omega_t^{-1}} \alpha^2 dt = \frac{1}{2\hbar^2\Omega_t^2}$ and $\nabla \mathcal{H}_1 = -\frac{1}{2}m\Omega_t^2 q \begin{bmatrix} x \\ -y \end{bmatrix}$.

Introducing the standard creation and annihilation operators

$$a_k^\dagger = \frac{1}{2\hbar} \left(\sqrt{m\omega_r} k - \frac{i}{\sqrt{m\omega_r}} p_k \right) \quad k = x, y$$

$$\text{and} \quad a_k = \frac{1}{2\hbar} \left(\sqrt{m\omega_r} k + \frac{i}{\sqrt{m\omega_r}} p_k \right)$$

yields

$$\mathcal{H} = \hbar\omega_r(a_x^\dagger a_x + a_y^\dagger a_y + 1) + \frac{i}{2}\hbar\omega_c(a_x^\dagger a_y - a_y^\dagger a_x), \quad (15)$$

i.e. a Hamiltonian for which x and y components are coupled with $\omega_c = eB/m$. This coupling can easily be resolved by introducing new creation and annihilation operators

$$a_+ = \frac{1}{\sqrt{2}}(a_x + ia_y) \quad \text{and} \quad a_- = \frac{1}{\sqrt{2}}(a_x - ia_y), \quad (16)$$

in terms of which the Hamiltonian reads

$$\begin{aligned} \mathcal{H} &= \hbar \left(\omega_r + \frac{1}{2}\omega_c \right) \left(a_+^\dagger a_+ + \frac{1}{2} \right) \\ &\quad + \hbar \left(\omega_r - \frac{1}{2}\omega_c \right) \left(a_-^\dagger a_- + \frac{1}{2} \right). \end{aligned} \quad (17)$$

That is, analogously to the classical case, there are two decoupled modes with shifted frequency $\omega_r \pm \frac{1}{2}\omega_c$, and the motion in z -direction is unaffected by the magnetic field.

5 Discussion and conclusion

In summary, we have proposed to encode quantum information in nuclear spins of trapped atomic ions and considered the feasibility of nuclear spin quantum information processing using trapped $^{171}\text{Yb}^+$ ions in a linear ion trap. Employing both nuclear and electron spins provides not only the combination of robust storage of quantum information with efficient quantum gating, but also a good way to suppress the undesired coupling between electron spins. The discussion of possible methods to generate the required magnetic field indicates that this scheme is feasible with currently or near-future available ion-trap techniques.

This scheme could also be applied to other candidate ions, such as $^{43}\text{Ca}^+$ [11–13] or ^9Be [12,13]. Since the hyperfine coupling in those ions is much smaller than in $^{171}\text{Yb}^+$, it is possible to satisfy the high-field approximation using a lower magnetic field. On the other hand, because the nuclear spins of those ions are not 1/2 (i.e. $^{43}\text{Ca}^+$ with $I = 7/2$ and ^9Be with $I = 3/2$), it would be more complicated to encode and manipulate qubits in nuclear spins. For example, as studied in [11], the nuclear spin flipping

operation would be more complex and take a relatively longer time. Particularly, when x and y terms of the hyperfine coupling are considered in the Hamiltonian, a very high magnetic field is required to obtain the desired fidelity. Using the similar calculation for the CONTIS gate for $7/2$ nuclear spin $^{43}\text{Ca}^+$ in [11], we have found that 5 T magnetic field are necessary to get an effective operation as good as that in the present paper for $^{171}\text{Yb}^+$. For $^9\text{Be}^+$, at least 1 T magnetic field is needed to reach a good high-field approximation.

In addition, without the magnetic field gradient, our scheme would still work using laser light for the electronic spin operations using the Cirac-Zoller model [14] or Mølmer-Sørensen model [15]. Due to involvement of nuclear spins, more qubits could be employed in the system with the same numbers of ions trapped compared to previous schemes using only electron spins.

This work is supported by National Natural Science Foundation of China under Grant Nos. 10774163 and 10974225, by the National Fundamental Research Program of China under Grant No. 2006CB921203, by the Deutsche Forschungsgemeinschaft, the EU STREP PICC, and secunet AG.

References

- L.M.K. Vandersypen, I.L. Chuang, *Rev. Mod. Phys.* **76**, 1037 (2004)
- M.V.G. Dutt, L. Childress, L. Jiang, E. Togan, J. Maze, F. Jelezko, A.S. Zibrov, P.R. Hemmer, M.D. Lukin, *Science* **316**, 1312 (2007)
- J. Du, N. Xu, X. Peng, P. Wang, S. Wu, D. Lu, *Phys. Rev. Lett.* **104**, 030502 (2010)
- X. Peng, J. Zhang, J. Du, D. Suter, *Phys. Rev. Lett.* **103**, 140501 (2009)
- B.E. Kane, *Nature* **393**, 133 (1998)
- W. Harneit, C. Meyer, A. Weidinger, D. Suter, J. Twamley, *Phys. Stat. Sol. B* **233**, 453 (2002)
- D. Suter, K. Lim, *Phys. Rev. A* **65**, 052309 (2002)
- J.J. Bollinger, D.J. Heinzen, W.H. Itano, S.L. Gilbert, D.J. Wineland, *IEEE Trans. Instrum. Meas.* **40**, 126 (1991)
- P. Neumann, N. Mizuochi, F. Rempp, P. Hemmer, H. Watanabe, S. Yamasaki, V. Jacques, T. Gaebel, F. Jelezko, J. Wrachtrup, *Science* **320**, 1326 (2008)
- V. Jacques, P. Neumann, J. Beck, M. Markham, D. Twitchen, J. Meijer, F. Kaiser, G. Balasubramanian, F. Jelezko, J. Wrachtrup, *Phys. Rev. Lett.* **102**, 057403 (2009)
- M. Feng, Y.Y. Xu, F. Zhou, D. Suter, *Phys. Rev. A* **79**, 052331 (2009)
- For instance, R. Blatt, D. Wineland, *Nature* **453**, 1008 (2008)
- J. Home, D. Hanneke, J. Jost, J. Amini, D. Leibfried, D. Wineland, *Science*, **325**, 1227 (2009)
- J.I. Cirac, P. Zoller, *Phys. Rev. Lett.* **74**, 4091 (1995)
- A. Sørensen, K. Mølmer, *Phys. Rev. Lett.* **82**, 1971 (1999)
- M. Johanning, A. Braun, N. Timoney, V. Elman, W. Neuhauser, C. Wunderlich, *Phys. Rev. Lett.* **102**, 073004 (2009)
- F. Mintert, C. Wunderlich, *Phys. Rev. Lett.* **87**, 257904 (2001)
- F. Mintert, C. Wunderlich, *Phys. Rev. Lett.* **91**, 029902 (2003)
- D. Mc Hugh, J. Twamley, *Phys. Rev. A* **71**, 012315 (2005)
- C. Wunderlich, in *Laser Physics at the Limit*, edited by D.M.H. Figger, C. Zimmermann (Springer, Berlin, 2002), p. 26171
- C. Wunderlich, C. Balzer, *Adv. At. Mol. Opt. Phys.* **49**, 293 (2003)
- C. Ospelkaus, C.E. Langer, J.M. Amini, K.R. Brown, D. Leibfried, D.J. Wineland, *Phys. Rev. Lett.* **101**, 090502 (2008)
- S.X. Wang, J. Labaziewicz, Y. Ge, R. Shewmon, I.L. Chuang, *Appl. Phys. Lett.* **94**, 094103 (2009)
- R. Ozeri, W.M. Itano, R.B. Blakestad, J. Britton, J. Chiaverini, J.D. Jost, C. Langer, D. Leibfried, R. Reichle, S. Seidelin, J.H. Wesenberg, D.J. Wineland, *Phys. Rev. A* **75**, 042329 (2007)
- M. Loewen, C. Wunderlich, *Verhandl. DPG*, **39** (2004)
- C. Balzer, A. Braun, T. Hannemann, C. Paape, M. Ettl, W. Neuhauser, C. Wunderlich, *Phys. Rev. A* **73**, 041407(R) (2006)
- D. Kielpinski, M. Cetina, J.A. Cox, F.X. Kärtner, *Opt. Lett.* **31**, 757 (2006)
- T. Hannemann, D. Reiss, C. Balzer, W. Neuhauser, P.E. Toschek, C. Wunderlich, *Phys. Rev. A* **65**, 050303 (2002)
- P. Maunz, D.L. Moehring, S. Olmschenk, K.C. Younge, D.N. Matsukevich, C. Monroe, *Nature Phys.* **3**, 538 (2007)
- M. Cetina, A. Grier, J. Campbell, I. Chuang, V. Vuletic, *Phys. Rev. A* **76**, 4 (2007)
- R. Huesmann, Ch. Balzer, Ph. Courteille, W. Neuhauser, P.E. Toschek, *Phys. Rev. Lett.* **82**, 1611 (1999)
- M. Johanning, A. Braun, D. Eiteneuer, Ch. Paape, Ch. Balzer, W. Neuhauser, Ch. Wunderlich, [arXiv:0712.0969v2](https://arxiv.org/abs/0712.0969v2) [physics.atom-ph] (2010)
- H. Wunderlich, C. Wunderlich, K. Singer, F. Schmidt-Kaler, *Phys. Rev. A* **79**, 052324 (2009)
- R. Folman, P. Krüger, J. Schmiedmayer, J. Denschlag, C. Henkel, *Adv. At. Mol. Opt. Phys.* **48**, 263 (2002)
- J. Fortagh, C. Zimmermann, *Rev. Mod. Phys.* **79**, 235 (2007)
- S. Groth, P. Krüger, S. Wildermuth, R. Folman, T. Fernholz, J. Schmiedmayer, D. Mahalu, I. Bar-Joseph, *Appl. Phys. Lett.* **85**, 2980 (2004)
- M.N. Wilson, *Superconducting magnets* (Clarendon Press, Oxford, 1983)
- J.M.D. Coey, T.R. Ní Mhíocháin, *High Magnetic Fields* (World Scientific Publishing, 2003), p. 35
- D.R. Lide, *CRC Handbook of Chemistry and Physics*, 88th edn. (CRC Press, 2008)
- J.M.D. Coey, T.R. Ní Mhíocháin, *High Magnetic Fields*, in *Permanent Magnets* (World Scientific Publishing, 2003)
- K. Halbach, *Nucl. Instrum. Methods* **169**, 1 (1980)
- H.A. Leupold, *Rare-earth Iron Permanent Magnets* (Oxford University Press, 1996), p. 380
- O. Cugat, F. Bloch, *IEEE Trans. Magn.* **34**, 2465 (1998)
- M. Sagawa, S. Fujimura, H. Yamamoto, Y. Matsuura, K. Hiraga, *IEEE Trans. Magn.* **20**, 1584 (1984)
- T. Tanaka, T. Hara, T. Bizen, T. Seike, R. Tsuru, X. Marechal, H. Hirano, M. Morita, H. Teshima, S. Nariki, N. Sakai, I. Hirabayashi, M. Murakami, H. Kitamura, *New J. Phys.* **8**, 16 (2006)
- P.K. Ghosh, *Ion Traps* (Clarendon Press, Oxford, 1995)
- F.G. Major, V.N. Gheorghie, G. Werth, *Charged Particle Traps* (Springer, Berlin, 2005)